Ferminoic Physics in Dipolariton Condensates

Jung-Jung Su,[1,2,3,*] Na Young Kim,[2] Yoshihisa Yamamoto,[1,2] and Allan H. MacDonald[4]
[1]*National Institute of Informatics, 2-1-2 Hitotsubashi, Chiyoda-ku, Tokyo 101-8430, Japan*
[2]*Edward L. Ginzton Laboratory, Stanford University, Stanford, California 94305-4085, USA*
[3]*Department of Electrophysics, National Chiao Tung University, Hsinchu 300, Taiwan*
[4]*Department of Physics, University of Texas at Austin, Austin, Texas 78712, USA*
(Received 19 February 2013; published 17 March 2014)

An exciton polariton is an extremely light bosonic quasiparticle that is composed of an exciton and a photon. We report on a theoretical study of exciton-polariton condensation in a system with tunnel-coupled quantum wells. Because their excitons can carry an electric dipole moment, these systems have been referred to as *dipolariton* condensates. We use a fermionic mean-field theory that can address quantum well and other internal exciton degrees of freedom to describe the new physics present in dipolariton condensates. We find that the role of underlying fermonic degrees of freedom is enhanced and predict that metallic condensates can occur at high carrier densities.

DOI: 10.1103/PhysRevLett.112.116401 PACS numbers: 71.36.+c, 67.10.Db

Introduction.—During the past decade experimenters have been able to study the physics of electron-hole pair condensates [1] in a variety of distinct [2–4] quasi-two-dimensional [5] condensed matter systems. Among these, quantum Hall condensates [2] are distinguished by being in true thermodynamic equilibrium, making it possible to explore their anomalous macroscopic transport properties, while polariton condensates are distinguished by their dual light-matter character which makes it possible to probe the condensate wave function directly. Until recently, polaritons have always been formed by establishing coherence between light and bound states formed by electrons and holes in the same quantum well (QW). This Letter is motivated by a recent breakthrough [6] that realized *dipolaritons*, polaritons with a matter component that is in part spatially indirect. We show in this Letter that, if dipolariton condensation can be achieved, this advance could open up new physics.

Polariton condensates occur in planar microcavity systems containing $N \geq 1$ QWs. A polariton condensate can, in general, have excitonic contributions from the N spatially direct or from the $N(N-1)$ spatially indirect particle-hole pair channels. Since the exciton reservoir, which is the source of condensate particles, is purely direct, and cavity photons can excite only direct excitons, the spatially indirect channels can be accessed only by matter tunneling between QWs. The simplest system in which this tunneling process plays an essential role [6] contains two QWs in which one direct and one indirect exciton are strongly coupled by conduction-band electron tunneling [See Fig. 1(a)]. When the direct and indirect exciton energies are both close to resonance, the polariton matter component is a coherent sum of direct and indirect exciton contributions. Dipolariton condensates have tunable dipole-dipole interactions and, by establishing a role for electron tunneling, enrich the interplay between bosonic condensation and the fermonic degrees of freedom from which the bosons are formed. In the following, we describe a microscopic mean-field theory that directly captures these aspects of dipolariton condensate physics. We find that in the high-density limit, which has been attracting increasing attention among polariton condensate researchers [7–9], dipolariton condensate states can be gapless and, therefore, metallic.

Mean-field theory of the dipolariton condensate.—Dipolariton condensates are nonequilibrium steady states in which an exciton bath provides a source of particles, resonance between exciton and cavity mode excitations couples matter and light, and photon leakage provides a decay channel. We adopt the simplest possible model of the quasiequilibrium steady state by assuming that full thermalization is achieved between matter and light, possibly at an elevated temperature, with the density of excitations dependent on pumping power and on the cavity decay rates. We then employ a mean-field approach, similar to those described in Ref. [9], in which the many-particle state is approximated by the direct product of a photon coherent state and a matter Slater determinant. In this model, only the sum of the number of particle-hole pairs and the number of cavity photons, $n_X = n_{\rm ph} + (n_c + n_{\tilde{c}} + n_h)/2$, is conserved. Here, $n_{\rm ph}$, n_c, $n_{\tilde{c}}$, n_h are, respectively, the density of photons, electrons in the direct (c) and indirect ($\tilde{c}$) conduction bands, and holes in the valence (v) band [see Fig. 1(a)]. The steady state is determined by minimizing the total energy density

$$\epsilon_T = n_{\rm ph}(\omega - \mu_X) + \epsilon_{\rm mat}(\mu_X, \Omega). \quad (1)$$

Here, ω is the optical cavity frequency of the condensate [10], μ_X is the common chemical potential of cavity photons and particle-hole pairs, and $\epsilon_{\rm mat}$ is the matter

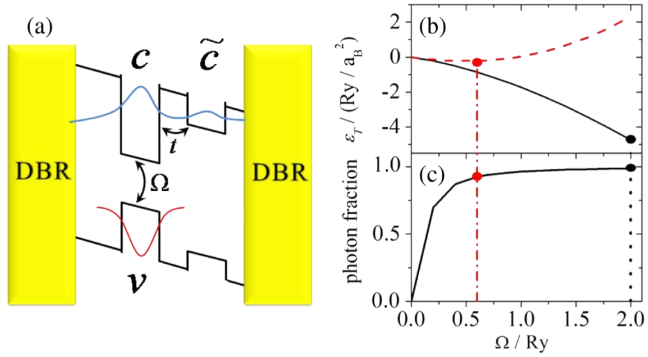

FIG. 1 (color online). (a) Schematic illustration of the simplest possible dipolariton system. Two quantum wells (QWs) are placed between a pair of distributed Bragg reflectors (DBRs) which form a cavity. The cavity mode is close to resonance with both direct excitons formed from conduction-valence (c-v) particle-hole pairs and indirect excitons formed from $\tilde{c}$-v particle-hole pairs. The blue curves and the red curves represent electron and hole wave functions, respectively. The QW system is designed so that exciton states other than those formed from c-v and $\tilde{c}$-v pairs are far off resonance with the active cavity mode. The c and v subbands are coupled by a photon field with Rabi coupling strength Ω, and the c and $\tilde{c}$ are coupled by tunneling with amplitude t. The energy difference dV between the c and $\tilde{c}$ subband energies can be tuned by applying a gate voltage to the structure. (b) Typical mean-field total energy density ϵ_T versus Ω for negative ($\Delta = 0^-$, black solid line) and positive ($\Delta = 0.1$ Ry, red dashed line) photon detuning. We use atomic energy units constructed from the GaAs reduced mass and static dielectric function so that 1 Ry = 4.67 meV. These results were calculated for model parameters $dV = 0$ Ry, $t = 1$ Ry, $\mu_X = -3.7$ Ry, and interlayer distance $d = 0.4a_B$. The minimum of ϵ_T at finite $\Omega = 0.6$ Ry (red circle) for $\Delta = 0.1$ Ry signals a polariton (mixed matter-light) condensate. (c) The photon fraction ($n_{\rm ph}/n_X$) versus Ω for the same parameters as in (b).

energy density including the contribution from coupling to photons. The Rabi coupling between excitons and photons Ω is proportional to $n_{\rm ph}^{1/2}$, as detailed below.

The matter energy can be determined by self-consistently solving a set of envelope-function Hartree-Fock equations. The single-particle part of the Hamiltonian is

$$H_M^0 = \sum_{\boldsymbol{k}} \left(\frac{\hbar^2 k^2}{2m_c} - \mu_X - \mu \right) c_{\boldsymbol{k}}^\dagger c_{\boldsymbol{k}} + \left(-\frac{\hbar^2 k^2}{2m_v} - \mu \right) v_{\boldsymbol{k}}^\dagger v_{\boldsymbol{k}} + \left(\frac{\hbar^2 k^2}{2m_c} - \mu_X - \mu - dV \right) \tilde{c}_{\boldsymbol{k}}^\dagger \tilde{c}_{\boldsymbol{k}}, \quad (2)$$

where $c_{\boldsymbol{k}}$, $\tilde{c}_{\boldsymbol{k}}$, and $v_{\boldsymbol{k}}$ are electron annihilation operators for c, $\tilde{c}$, and v bands. dV is the offset between c and $\tilde{c}$ subband energies. In Eq. (2) we have chosen the zero of energy for particle-hole excitations at the QW-confinement enhanced band gap. We have also introduced an additional Lagrange multiplier μ whose value is chosen to impose neutrality on the system, i.e., to set the number of conduction-band

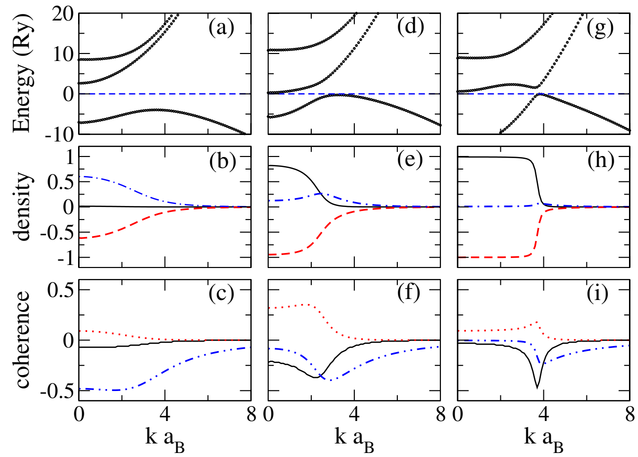

FIG. 2 (color online). Quasiparticle (QP) dispersion (top row), electron density (middle row), and interband coherence (bottom row) versus momentum for $\mu_X = -3.7$ Ry (BEC limit). The left-hand, middle, and right-hand columns correspond to $dV = 0$, 9.5, and 20 Ry. In the density plots, the black solid lines, blue dash-dotted lines, and red dashed lines correspond to the densities of $\tilde{c}$ and c electrons and v holes. In the coherence plots, the black solid lines, blue dash-double-dotted lines, and red dotted lines correspond to $\langle \tilde{c}|\rho|v\rangle$, $\langle c|\rho|v\rangle$, and $\langle \tilde{c}|\rho|c\rangle$. The results were calculated for $t = 1$ Ry, $\Omega = 2$ Ry, $\Delta = 0$, and quantum well separation $d = 0.4a_B$.

electrons in the system, summing over the two QWs, equal to the number of valence-band holes. As we discuss later, the presence of three quasiparticle (QP) bands in this model allows for the possibility of partial band filling at neutrality, and hence metallic behavior.

The dipolariton matter mean-field Hamiltonian has additional contributions due to interlayer tunneling, interactions between photons and matter, and Coulomb interactions:

$$H_{\rm int} = H_H + H_F + \sum_{\boldsymbol{k}} [\Omega c_{\boldsymbol{k}}^\dagger v_{\boldsymbol{k}} - t c_{\boldsymbol{k}}^\dagger \tilde{c}_{\boldsymbol{k}} + {\rm H.c.}], \quad (3)$$

where H.c. denotes the Hermitian conjugate of the two terms inside the bracket. The Hartree term $H_H = -2\pi e^2 d n_{\tilde{c}} \sum_{\boldsymbol{k}} (c_{\boldsymbol{k}}^\dagger c_{\boldsymbol{k}} + v_{\boldsymbol{k}}^\dagger v_{\boldsymbol{k}} - \tilde{c}_{\boldsymbol{k}}^\dagger \tilde{c}_{\boldsymbol{k}})$ captures energy shifts due to the dipoles carried by the indirect excitons. The exchange interaction term is $H_F = -\sum_{\boldsymbol{k},\boldsymbol{k}'} \langle b, \boldsymbol{k}; b', \boldsymbol{k}'|V_C|b, \boldsymbol{k}'; b', \boldsymbol{k}\rangle \langle b, \boldsymbol{k}'|\rho|b', \boldsymbol{k}\rangle b_{\boldsymbol{k}}^\dagger b'_{\boldsymbol{k}}$. Here, b, $b' = c$, $\tilde{c}$, v are band indices, V_C is the Coulomb interaction between electrons, and ρ is the density-matrix operator. As in the simpler spatially direct exciton case, exchange terms support interband coherence and capture the attractive interaction between conduction band electrons and valence band holes. The Rabi coupling terms in Eq. (3) are a consequence of the coupling of matter to the photon component of the exciton-polariton condensate. It is given by $\Omega = g n_{\rm ph}^{1/2}$, where $n_{\rm ph}$ is the photon component of the condensate and g is the electron-hole-pair–photon coupling constant. We choose [11] $g = 1$ Rya_B, where

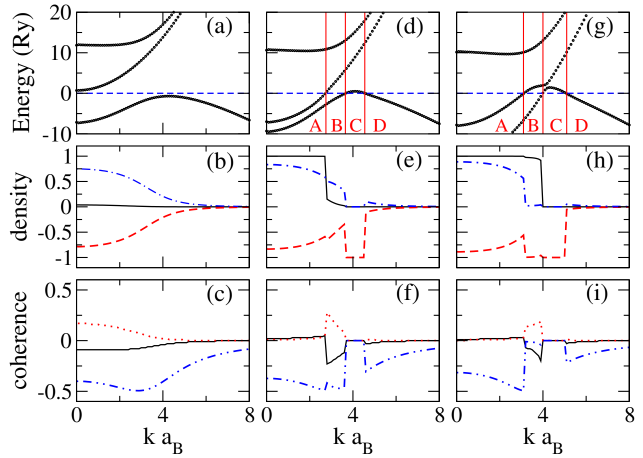

FIG. 3 (color online). Quasiparticle dispersion (top row), electron density (middle row), and interband coherence (bottom row) versus momentum for $\mu_X = 0$ (BCS limit). The curve legend is identical to that used in Fig. 2. In the QP dispersion plot, regions A, B, C, and D have 2, 1, 0, and 1 occupied QP bands. These calculations were performed for $\mu_X = 0$ and all other parameters set to the same values as in Fig. 2.

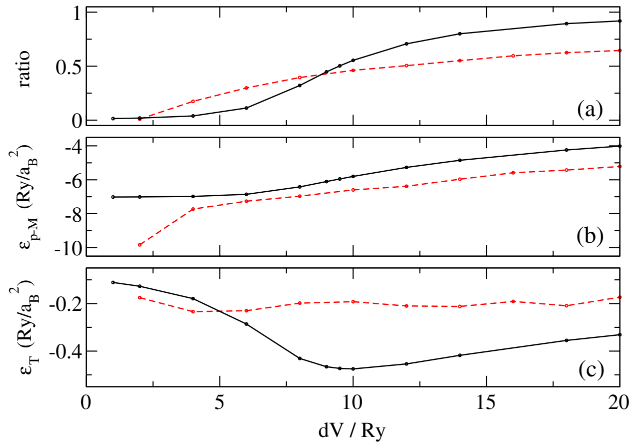

FIG. 4 (color online). Condensate character versus conduction band QW resonance detuning dV. (a) Indirect electron fraction $n_{\tilde{c}}/(n_c + n_{\tilde{c}})$ versus dV. (b) Photon-matter coupling energy density ϵ_{p-M} versus dV. (c) Tunneling energy density ϵ_T versus dV. The black solid lines refer to the BEC limit ($\mu_X = -3.7$ Ry) and the red dashed lines to the BCS limit ($\mu_X = 0.0$ Ry). All other parameters are the same as in Fig. 2.

a_B is the Bohr radius of free exciton in the explicit calculations described below. The strength of tunneling between c and $\tilde{c}$ states is characterized by the amplitude t. Because the interaction contributions to the matter mean-field Hamiltonian depend on the matter density matrix, they must be determined self-consistently as a function of μ_X and Ω. The solutions of these equations define QP bands that are dressed by electron-electron and electron-photon interactions and determine the fermionic properties of the dipolariton condensate. Typical results, summarized in Figs. 2 and 3 are discussed in detail below.

For $\Delta = \omega - \mu_X \leq 0$, incoherent conversion of matter into photons releases energy. Under this circumstance, the total energy per area of the photon-matter system ϵ_T is always minimized at the largest possible Ω. This is the normal laser case in which matter and light are not in equilibrium and our model of the steady state is inappropriate. Polariton condensates occur when $\Delta > 0$ and incoherent conversion of matter to photons requires energy. In this regime, the pure photon contribution to ϵ_T is positive and proportional to $n_{\rm ph} \propto \Omega^2$, whereas the matter contribution $\epsilon_{\rm mat}$ is negative and satisfies the Hellmann-Feynman theorem:

$$\frac{\partial \epsilon_{\rm mat}(\mu_X, \Omega)}{\partial \Omega} = \frac{1}{S} \sum_{\boldsymbol{k}} \langle c_{\boldsymbol{k}} v_{\boldsymbol{k}}^{\dagger} + \text{H.c.} \rangle, \qquad (4)$$

where S is the system area. If excitons are able to form a condensate without coupling to cavity photons, the right-hand side of Eq. (4) remains finite for $\Omega \to 0$, and the matter contribution to ϵ_T is therefore linear in Ω. A minimum in ϵ_T thus occurs for a partially excitonic and partially photonic finite Ω state. For example, as illustrated in Fig. 1, the minimum occurs at $\Omega = 0.6$ Ry for $\Delta = 0.1$ Ry. Typical total energy results in the low-exciton density Bose-Einstein condensation (BEC) limit ($\mu_X = -3.7$ Ry) are shown in the right-hand panel of Fig. 1. Importantly, if the matter response to Ω is strong enough, minima can occur at finite Ω even when an exciton condensate does not form at $\Omega = 0$.

Fermionic properties of dipolariton condensates.—Our mean-field theory is more reliable in predicting fermionic QP properties at a given value of Rabi coupling Ω than in predicting how the condensate is partitioned between photon and matter components. We focus our discussion of QP bands on two particular chemical potentials, $\mu_X = -3.7$ Ry and $\mu_X = 0.0$ Ry, which are representative of the BCS and BEC limits.

In the narrow QW model [12], the $\Omega = 0$ spatially direct dilute exciton chemical potential is reduced relative to the band gap by the two-dimensional hydrogenic ground state binding energy to $\mu_X = -4$ Ry. Because interlayer electron-hole interactions are weaker than intralayer interactions, the shift is smaller for indirect excitons. In the dilute limit, the two excitons therefore come into resonance at a positive value of dV that is dependent on the QW separation distance d for $\Omega = 0$ and $dV \in (0, 4$ Ry). As illustrated in Fig. 4(b), the magnitude of the interlayer tunnel energy $t \sum_{\boldsymbol{k}} \langle c_{\boldsymbol{k}}^{\dagger} \tilde{c}_{\boldsymbol{k}} + \text{H.c.} \rangle$ is maximized near resonance in the BEC limit, but is more weakly dependent on dV in the BCS limit [Fig. 4(c)]. The matter part of the polariton develops more indirect exciton character and the photon-matter coupling strength $|\Omega \sum_{\boldsymbol{k}} \langle c_{\boldsymbol{k}}^{\dagger} v_{\boldsymbol{k}} + \text{H.c.} \rangle|$ slowly weakens as dV is increased beyond the resonance value. These differences in condensate character are reflected in the QP energies and wave functions, as we explain in the following paragraphs.

Figure 2 plots the QP bands and both diagonal (density) and off-diagonal (interband coherence) density-matrix components for $\mu_X = -3.7$ Ry. Energies in these plots are given relative to the chemical potential μ, so negative energy bands are occupied. At $dV = 0$, the indirect excitons are above resonance and our results differ little from those obtained [7–9] previously for a simple polariton condensate. The single occupied band consists entirely of conduction and valence bands in the same QW. At $dV = 9.5$ Ry, we begin to see how fermionic physics limits the validity of the purely bosonic description of dipolariton condensates. In the condensed state, avoided crossings, marked by interband coherence peaks, occur at finite k between both the v band and both c and $\tilde{c}$ conduction bands. The occupied QP band is a coherent combination with substantial weights for all three constituents and a wave vector dependence that reflects a delicate interplay between Rabi, self-consistent exchange, and interlayer tunneling couplings. The matter part of the condensate is not properly viewed as being simply a coherent sum of direct and indirect exciton components. For still larger dV, the condensate crosses over toward a simple indirect-exciton state in which the c band plays a small role. Although reduced, coupling to light is surprisingly persistent. This behavior can be traced to $\sim t^2/dV$ perturbative mixing between the two conduction bands, which allows photons to support the avoided crossing gap and associated coherence between the valence band and the $\tilde{c}$ conduction band at the Fermi energy.

In the high-density BCS limit, illustrated in Fig. 3 by plotting results for $\mu_X = 0.0$, a fermionic description is required even away from resonance. At small dV we recover results close to those obtained in earlier microscopic studies of direct exciton BCS condensates [6,8,9]. Bare c and v bands cross at a finite wave vector where they have a Fermi level avoided crossing gap due to interaction induced coherence. As dV increases, the bottom of the $\tilde{c}$ band falls below the top of the valence band. Because there are two occupied bands at small $k \equiv |\boldsymbol{k}|$, neutrality requires that there be an equal area region in which no bands are occupied. (See the Supplemental Material for further remarks on the QP bands [13].) The end result is that three bands cross the Fermi energy, leading to a Fermi surface with three circular segments, two electronlike and one holelike. In Fig. 3(d) two QP bands are occupied in region A, which is a circle centered on $k = 0$. At larger k the annular regions B and C have one and zero occupied bands, respectively, while the rest of momentum space region (D) again has one occupied band. Contributions to the tunneling energy and to indirect exciton coherence energy come mainly from region B. In this parameter regime, condensation does not occur unless assisted by coupling to the cavity photon field. Direct exciton pairing is weakened, but metallic behavior is retained when dV is increased further.

Discussion.—Our theory is based on two approximations: a mean-field theory for fermionic interactions [7,9] and a quasiequilibrium approximation for the polariton steady state. The mean-field theory is known to give a qualitatively correct description of the BEC-BCS crossover [14] of direct QW excitons, but probably overestimates pairing strength in the BCS limit because it neglects screening effects. As in the simple exciton-polariton case, the quasiequilibrium ansatz is the more serious, and more difficult to remedy, although some progress as been made [15]. It requires that scattering rates among constituents exceed the rate of scattering in from the incoherent exciton reservoir and the rate of photon loss. These conditions are more closely satisfied in systems with high quality factor cavities. In the dipolariton case, the rate of electron tunneling between QWs must also be large, a requirement that can be achieved in III-V semiconductor systems simply by growing structures with small x or narrow $B_x\mathrm{III}_{1-x}\mathrm{V}$ tunnel barriers. (Here, B is the group III barrier material.) Electron tunneling amplitudes similar to the ones assumed in our illustrative calculations have been realized experimentally in Ref. [6]. For structures of this type the quasiequilibrium approximation we employ should be as reliable in dipolariton systems as it is in the single QW case where it has been employed in the past. Our theory is of little value in predicting the Rabi coupling strengths or photon fractions of polariton states obtained at a given coupling strength, but it is qualitatively reliable for understanding condensate properties at given Rabi coupling strengths and matter densities.

Because it is formulated in terms of electronic degrees of freedom, our theory can be extended to consider both vertical and in-plane two-dimensional electron transport. The recent realization of electrical-injection exciton-polariton condensation [16] is promising in this respect. The most intriguing prediction of our theory is that dipolariton condensates can be two-dimensional metals in which the exciton binding energy vanishes but coherence is maintained. Although dipolariton systems generally tend less strongly toward coherence at $\Omega = 0$, i.e., pure exciton condensation tends not to occur, the rate at which coherence is induced by coupling to photons is large. For the parameters of Fig. 3, for example, the total energy at $\Omega = 2$ Ry is lower than the energy at $\Omega = 0$ for $\Delta < 0.2$ Ry. The combination of coherence with metallic conductivity is unprecedented in exciton-polariton condensates. If this state is realized experimentally, it would open up a new class of photoconductive phenomena.

J.-J. S., N. Y. K., and Y. Y. were supported by Navy/SPAWAR Grant No. N66001-09-1-2024 and by the Japan Society for the Promotion of Science (JSPS) through its "Funding Program for World-Leading Innovative R&D on Science and Technology (FIRST Program)." A. H. M. was supported by Welch Foundation Grant No. TBF1473 and by DOE Division of Materials Sciences and Engineering Grant No. DE-FG03-02ER45958.

*jungjsu@nctu.edu.tw

[1] J. M. Blatt, K. W. Böer, and W. Brandt, Phys. Rev. **126**, 1691 (1962); L. V. Keldysh and A. N. Kozlov, Sov. Phys. JETP **27**, 521 (1968).

[2] H. A. Fertig, Phys. Rev. B **40**, 1087 (1989); J. P. Eisenstein and A. H. MacDonald, Nature (London) **432**, 691 (2004).

[3] J. Kasprzak *et al.*, Nature (London) **443**, 409 (2006); S. Christopoulos *et al.*, Phys. Rev. Lett. **98**, 126405 (2007); R. Balili, V. Hartwell, D. Snoke, L. Pfeiffer, and K. West, Science **316**, 1007 (2007); A. Kavokin and G. Malpuech, *Cavity Polaritons* (Elsevier, New York, 2003); D. Snoke and P. Littlewood, Phys. Today **63**, 8, 42 (2010); H. Deng, H. Haug, and Y. Yamamoto, Rev. Mod. Phys. **82**, 1489 (2010).

[4] A. A. High, J. R. Leonard, M. Remeika, L. V. Butov, M. Hanson, and A. C. Gossard, Nano Lett. **12**, 2605 (2012).

[5] N. B. Brandt and S. M. Chudinov, J. Low Temp. Phys. **8**, 339 (1972); Y. E. Lozovik and V. I. Yudson, JETP Lett. **22**, 274 (1975); L. V. Butov, J. Phys. Condens. Matter **19**, 295202 (2007).

[6] P. Cristofolini, G. Christmann, S. I. Tsintzos, G. Deligeorgis, G. Konstantinidis, Z. Hatzopoulos, P. G. Savvidis, and J. J. Baumberg, Science **336**, 704 (2012); G. Christmann, A. Askitopoulos, G. Deligeorgis, Z. Hatzopoulos, S. I. Tsintzos, P. G. Savvidis, and J. J. Baumberg, Appl. Phys. Lett. **98**, 081111 (2011).

[7] For the fermionic mean-field theory for exciton, see, for example, C. Comte and P. Nozieres, J. Phys. (Paris) **43**, 1069 (1982); X. Zhu, P. B. Littlewood, M. S. Hybertsen, and T. M. Rice, Phys. Rev. Lett. **74**, 1633 (1995); X. Zhu, M. S. Hybertsen, and P. B. Littlewood, Phys. Rev. B **54**, 13 575 (1996); H. Min, R. Bistritzer, J.-J. Su, and A. H. MacDonald, Phys. Rev. B **78**, 121401(R) (2008).

[8] J. Keeling, P. R. Eastham, M. H. Szymanska, and P. B. Littlewood, Phys. Rev. Lett. **93**, 226403 (2004); J. Keeling, P. R. Eastham, M. H. Szymanska, and P. B. Littlewood, Phys. Rev. B **72**, 115320 (2005); M. Yamaguchi, K. Kamide, R. Nii, T. Ogawa, and Y. Yamamoto, Phys. Rev. Lett. **111**, 026404 (2013).

[9] P. B. Littlewood, P. R. Eastham, J. M. J. Keeling, F. M. Marchetti, B. D. Simons, and M. H. Szymanska, J. Phys. Condens. Matter **16**, S3597 (2004), Sec. 4.1; F. M. Marchetti, B. D. Simons, and P. B. Littlewood, Phys. Rev. B **70**, 155327 (2004); T. Byrnes, T. Horikiri, N. Ishida, and Y. Yamamoto, Phys. Rev. Lett. **105**, 186402 (2010); K. Kamide and T. Ogawa, Phys. Rev. B **83**, 165319 (2011).

[10] The planar condensate is assumed to form at zero wave vector. Collective modes of the condensate, which will have the standard linear dispersion at long wavelengths and reflect the light polariton mass, are not discussed in this Letter.

[11] The coupling constant g is related to the coupling constant g_B which appears in the bosonic exciton-polariton theory by $g = g_B/C$, where $C = \sum_k \langle c_k^\dagger v_k \rangle / (S \sum_k |\langle c_k^\dagger v_k \rangle|^2)^{1/2}$ and $S \sim 1\ \mu\text{m}^2$ is the area of the 2D system. Since g_B varies from 1 to 3 Ry in the current experiments and $C \sim 3a_B^{-1}$ calculated in the dilute limit, we choose $g = 1\ \text{Ry}a_B$ in our explicit calculations.

[12] G. Bastard, E. E. Mendez, L. L. Chang, and L. Esaki, Phys. Rev. B, **26**, 1974 (1982); **28**, 3241 (1983).

[13] See Supplemental Material at http://link.aps.org/supplemental/10.1103/PhysRevLett.112.116401 for the details of quasiparticle bands.

[14] M. Randeria, J.-M. Duan, and L.-Y. Shieh, Phys. Rev. Lett. **62**, 981 (1989); , Phys. Rev. B **41**, 327 (1990).

[15] J. Keeling and N. Berloff, Contemp. Phys. **52**, 131 (2011)

[16] C. Schneider *et al.*, Nature (London) **497**, 348 (2013); P. Bhattacharya, B. Xiao, A. Das, S. Bhowmick, and J. Heo, Phys. Rev. Lett. **110**, 206403 (2013).